Saudi Pharmaceutical Journal 32 (2024) 102051

HOSTED BY

Contents lists available at ScienceDirect

Saudi Pharmaceutical Journal

journal homepage: www.sciencedirect.com

Development of a microcantilever-based biosensor for detecting Programmed Death Ligand 1

Tajweed Neairat [a], Mahmoud Al-Gawati [a,b], Qura Tul Ain [c], Abdulaziz K. Assaifan [b,d], Aws Alshamsan [e], Abdulaziz Alarifi [f,g], Abdullah N. Alodhayb [a,b,*], Khalid E. Alzahrani [a,b,*], Hamad Albrithen [a,b,*]

[a] Department of Physics and Astronomy, College of Science, King Saud University, Riyadh 11451, Saudi Arabia
[b] Biological and Environmental Sensing Research Unit, King Abdullah Institute for Nanotechnology, King Saud University, Riyadh, Saudi Arabia
[c] Department of Physics, The Women University Multan, Khawajabad, Multan, Pakistan
[d] Department of Biomedical Technology, College of Applied Medical Science, King Saud University, Riyadh, Saudi Arabia
[e] Department of Pharmaceutics, College of Pharmacy, King Saud University, Riyadh, Saudi Arabia
[f] Department of Basic Sciences, College of Science and Health Professions, King Saud bin Abdulaziz University for Health Sciences, Riyadh, Saudi Arabia
[g] King Abdullah International Medical Research Center, Riyadh, Saudi Arabia

ARTICLE INFO

Keywords:
Biosensor
Program Death Ligand 1
Cantilever-based sensors
AFM

ABSTRACT

The ongoing global concern of cancer worldwide necessitates the development of advanced diagnostic and therapeutic strategies. The majority of recent detection strategies involve the employment of biomarkers. A critical biomarker for cancer immunotherapy efficacy and patient prognosis is Programmed Death Ligand 1 (PD-L1), which is a key immune checkpoint protein. PD-L1 can be particularly linked to cancer progression and therapy response. Current detection methods, such as enzyme-linked immunosorbent assay (ELISA), face limitations like high cost, time consumption, and complexity. This study introduces a microcantilever-based biosensor designed for the detection of soluble PD-L1 (sPD-L1), which has a specific association with PD-L1. The biosensor utilizes anti-PD-L1 as the sensing layer, capitalizing on the specific binding affinity between anti-PD-L1 and sPD-L1. The presence of the sensing layer was confirmed through Atomic Force Microscopy (AFM) and contact angle measurements. Binding between sPD-L1 and anti-PD-L1 induces a shift in the microcantilever's resonance frequency, which is proportional to the PD-L1 concentration. Notably, the resonance frequency shift demonstrates a robust linear relationship with the increasing biomarker concentration, ranging from 0.05 ng/ml to 500 ng/ml. The detection limit of the biosensor was determined to be approximately 10 pg/ml. The biosensor demonstrates excellent performance in detecting PD-L1 with high specificity even in complex biological matrices. This innovative approach not only provides a promising tool for early cancer diagnosis but also holds potential for monitoring immunotherapy efficacy, paving the way for personalized and effective cancer treatments.

1. Introduction

Globally, cancer remains a leading cause of death, presenting significant obstacles in both its treatment and diagnosis (Bray et al., 2018, Ferlay et al., 2021, Mansouri et al., 2021). Immune-checkpoint blockade therapies, known for their effectiveness in treating various types of cancer, target proteins such as programmed death-1 (PD-1) and programmed death ligand-1 (PD-L1), which are utilized by cancer cells to escape immune detection (Mahoney et al., 2015, Patel and Kurzrock, 2015). PD-L1 binds to the PD-1 receptor on T-cells, inhibiting their activity and allowing cancer cells to avoid immune responses. These therapies focus on disrupting the PD-1/PD-L1 interaction, thus reactivating immune cells to target and destroy cancer cells (Feng et al., 2017, Jiang et al., 2019). PD-L1 expression in tumor cells is being investigated as a potential biomarker for predicting therapeutic responses. PD-1 and PD-L1, while primarily membrane proteins, also exist in soluble forms, such as soluble PD-1 (sPD-1) and soluble PD-L1 (sPD-L1). In cancers that respond to PD-1/PD-L1 blockade treatments, high

* Corresponding authors at: Department of Physics and Astronomy, College of Science, King Saud University, Riyadh 11451, Saudi Arabia.
E-mail addresses: aalodhayb@ksu.edu.sa (A.N. Alodhayb), alzkhalid@KSU.EDU.SA (K.E. Alzahrani), brithen@ksu.edu.sa (H. Albrithen).

https://doi.org/10.1016/j.jsps.2024.102051
Received 19 January 2024; Accepted 25 March 2024
Available online 27 March 2024

levels of soluble PD-L1 (sPD-L1) in plasma are often linked to a worse prognosis (Frigola et al., 2011, Ding et al., 2017, Kruger et al., 2017, Chang et al., 2019). Additionally, the considerable cost and potential autoimmune side effects of PD-L1 targeting drugs underscore the need for selectively identifying patients who will most likely benefit from such treatments. The concentration of sPD-L1 could be an indicator of the PD-L1 expression in cancer cells. Consequently, the presence of sPD-1 and sPD-L1 in serum or plasma is receiving increased attention as a crucial biomarker in assessing the efficacy of immunotherapy, aiding in the selection of suitable treatments, predicting patient outcomes, and understanding the prognosis of various cancers (Patel and Kurzrock, 2015, Festino et al., 2016, Yang et al., 2021). Consequently, there is a pressing need to develop sensitive, user-friendly, and cost-effective technologies for the direct detection of PD-L1.

Currently, the primary method for detecting sPD-1 and sPD-L1 predominantly relies on enzyme-linked immunosorbent assay (ELISA) (Chen et al., 2011). However, this method encounters several practical limitations, such as the need for skilled personnel, time-consuming handling processes, and high costs. Reza et al. described (Reza et al., 2019) a method for detecting soluble immune checkpoints using a Surface Enhanced Raman Scattering (SERS) microfluidic platform. This approach effectively identified clinically relevant soluble immune checkpoints PD-1, PD-L1, and LAG-3 in concentrations as low as 100 fg/mL. The detection range for this method covers varying concentrations of specific biomarkers. The serum samples tested contained PD-1 in the range of 100 fg/mL to 1 ng/mL, PD-L1 in the range of 50 fg/mL to 100 pg/mL, and LAG-3 in the range of 100 fg/mL to 1 ng/mL. An additional detection method utilizing a surface plasmon resonance (SPR) sensor was established for sPD-L1. This detection relies on the unique and strong binding affinity of the Specific Intracellular Binding Peptide (SIBP) for the intracellular region of sPD-L1. The SPR sensor demonstrated a broad dynamic range, effectively detecting sPD-L1 at concentrations ranging from 10 ng/mL to 2000 ng/mL. The detection threshold for sPD-L1 was established at 1.749 ng/mL (Hu et al., 2021). In a study by Xing et al. (2022), a differential pulse voltammetry electrochemical method was employed for the detection of sPD-1 and sPD-L1. This method enabled the immunosensor to detect sPD-1 and sPD-L1 in the range of 50 pg/mL to 50 ng/mL and in the range of 5 pg/mL to 5 ng/mL, respectively. The limits of detection for sPD-1 and sPD-L1 were determined to be 10 pg/mL and 5 pg/mL, respectively. This detection platform demonstrated its capability by successfully detecting sPD-1 and sPD-L1 in plasma using both the enzyme-linked immunosorbent assay and the immunosensor, indicating its promising application potential. A paper-based microfluidic electrochemical aptasensor was described for the detection of PD-L1 (Xing et al., 2021). This sensor integrates a reaction cell, a three-electrode system, and utilizes differential pulse voltammetry for electrochemical measurement. The detection limit of this method is 10 pg/mL, and it has a linear detection range between 10 pg/mL and 2.5 ng/mL. In another study, modified gold-coated magnetic nanoparticles, functioning as “dispersible electrodes” was used as electrochemical detection mechanism of PD-L1 directly in undiluted whole blood specimens(RáGonšales and JustináGooding, 2021). The method exhibits a remarkably minimal detection limit of 15 attomolar coupled with a rapid response time of 15 min. However, it’s noted that the uncertainties were greater when working in whole blood compared to the buffer, reflecting the increased complexity and potential interferences present in the blood matrix. A gold-coated Quartz Tuning Fork (QTF) was introduced as a biosensor for detecting sPD-L1 protein (Algwati et al., 2023). This biosensor, functionalized with PD-L1 antibodies, detects sPD-L1 by measuring changes in resonance frequency caused by antibody-protein binding. The sensor can detect PD-L1 concentrations ranging from 50 pg/ml to 0.5 μg/ml with a notably low limit of detection of 8.26 pg/ml.

Microcantilever-based biosensors, renowned for their rapid response, high sensitivity, ease of use, and cost efficiency, are steadily gaining recognition across various detection fields (Longo et al., 2013, Gopinath et al., 2015, Kim et al., 2015, Alzahrani et al., 2021, Alzahrani et al., 2023a,b). They consist of tiny, flexible beams anchored at one end, leaving the opposite end free to come into contact with adjacent materials. Utilizing microcantilevers for sensing requires the alteration of their surface with a specific recognition layer. The interaction of a targeted analyte with the cantilever’s surface triggers an observable mechanical response such as bending or a frequency shift. These reactions are typically measured via optical or electrical methods, with the intensity of the response serving as an indicator of the substance’s concentration or presence. A biosensor based on a cantilever array was employed for identifying biomarkers associated with liver cancer(Wang, Wang et al., 2015). Each cantilever in this sensor is equipped with a micro-cavity at its tip, specifically intended for the targeted immobilization of antibodies. The sensor boasts a low detection limit, capable of identifying the liver cancer biomarker alpha-fetoprotein (AFP) at a concentration of 7.6 pg/ml. Another method, based on microcantilever, was utilized for the detection of circulating tumor cells, particularly those originating from breast cancer (Etayash et al., 2015). In this approach, the microcantilever is functionalized with a distinct peptide, which exhibits notable deflection upon binding with cancer cells, thereby effectively differentiating them from noncancerous cells. The study reported a detection limit of 50 to 100 cancer cells per milliliter of blood samples. Ricciardi et al. (2010) designed a microcantilever-based biosensor array to detect Angiopoietin-1, a marker potentially indicating tumor progression. This method utilizes a cantilever-based system, which has been shown to be a highly sensitive mass detector with enhanced precision and specificity. The system’s repeatability and reproducibility were confirmed through the combination of results from the first and second modes of vibration. Two bio-designs, receptor-based and antibody-based, were optimized for detecting Angiopoietin-1 masses in the order of a few hundred picograms with less than 0.5 % of relative uncertainty.

In this study, we introduce a microcantilever-based biosensor that employs anti-PD-L1 as the sensing layer of sPD-L1, providing a promising tool for cancer diagnosis and monitoring the efficacy of immunotherapy treatments. This approach represents a significant evolution from our previous work (Algwati et al., 2023), which utilized a quartz tuning fork as the detection mechanism. Both techniques fall under the umbrella of mechanical methods, yet they offer distinct advantages and cater to different aspects of biosensing technology. The quartz tuning fork-based technique in our previous work was pivotal in demonstrating the viability of mechanical detection methods for biomarkers. However, the microcantilever-based approach in our current study introduces several enhancements. The microcantilever’s compact design enables integration into smaller devices, making it ideal for lab-on-a-chip applications. This miniaturization is crucial for developing portable and accessible diagnostic tools. Moreover, the ability to integrate microcantilevers with microfluidic systems allows for efficient sample handling and processing. This compatibility significantly enhances the utility of our biosensor by enabling the use of very small sample volumes, which is especially beneficial in scenarios where sample availability is limited. Unlike quartz tuning forks that typically measure changes in frequency, microcantilevers offer the additional capability to measure changes in deflection. This dual functionality not only enriches the data obtained from the sensor but also provides greater flexibility in detecting a wide range of biomolecular interactions. The ability to measure deflection allows for the detection of minute forces and mass changes on the sensor surface, enhancing the sensitivity and specificity of the biosensor.

2. Material and methods

2.1. Apparatus and reagents

All reagents including cysteamine, glutaraldehyde, and PBS were obtained from Sigma-Aldrich Corporation (Sigma, St. Louis, MO, USA).

Rabbit anti-human PD-L1 antibody (anti-PD-L1) and PD-L1 protein were provided by Moleqcule-On, New Zealand. The Atomic force microscopy (AFM) cantilevers used are designed for tapping mode imaging with resonance frequencies at 320 kHz and nominal tip with a radius of approximately 7 nm. AFM images and measurements were recorded with AFM Multimode (Bruker, USA). The surface wettability was assessed using the Attension T330 contact angle measuring system from Biolin Scientific. The change in the microcantilever's frequency was monitored using a detection system based on optical technology, integrated with the Picomeasure (PM3) system from FOURIEN, Canada. In this system, a laser beam is focused on the free end of the microcantilever and the reflected beam is directed to a position sensitive detector (PSD). The system has been extensively discussed in details in (Alzahrani et al., 2021, Alzahrani et al., 2023a,b). Arrays of microcantilevers, each consisting of eight identical cantilevers (500 μm long, 90 μm wide, and 1 μm thick) were purchased from Micromotive-company, Germany.

2.2. Sensor preparation

The microcantilever was modified, as illustrated in Fig. 1, with 5 nm layer of chromium followed by a 40 nm layer of gold deposited onto the microcantilever through evaporation using a vacuum thermal evaporation system. In this configuration, a gold layer acts as the substrate for the immobilization of cysteamine layer. The microcantilevers were cleaned with Piranha solution, then thoroughly rinsed several times with MilliQ water (18 MΩ) and ethanol, and subsequently air-dried. The microcantilevers were immersed in a 10 mM ethanolic solution of cysteamine for 60 min, rinsed with ethanol, and then air-dried. Next, they were incubated for another 60 min in a solution of 2.5 % glutaraldehyde dissolved in PBS buffer, followed by repeated rinses with deionized (DI) water. Consequently, the microcantilever is capable of binding with the anti-PD-L1. The anti-PD-L1 were immobilized onto the surface by incubating the microcantilevers with a 10 μg/mL PD-L1 antibody in PBS buffer for 60 min, followed by a rinse with deionized DI water. Finally, to deactivate any remaining active groups on the surface, the microcantilevers were immersed in a 1 μM solution of ethanolamine (Reinemann et al., 2009).

Following the functionalization of the microcantilever with the anti-PD-L1, it was placed into a specially fabricated measurement cell. The selected concentration of the target molecule (PD-L1) was then introduced into the cell to interact with the anti-PD-L1 immobilized on the microcantilever's surface and left for 15 min, followed by a rinse with deionized water. All experiments were conducted at room temperature and at a pH of 7.4, closely mirroring the pH of human blood. PBS is commonly utilized in proof-of-concept experiments as it effectively simulates the conditions of blood media. The microcantilever's resonance frequency was monitored in-situ. The change in resonance frequency was determined by subtracting the initial frequency of the microcantilever modified with the anti-PD-L1.

2.3. Measurements

The surface of microcantilevers was analyzed using Atomic Force Microscopy (AFM) before and after applying the probe layer. Images were captured in air at room temperature employing tapping mode. The surface roughness was determined by calculating the root-mean-square roughness (σ_R) over an area of 5 μm × 5 μm. Variations in surface roughness serve as indicators for the formation of the probe layer. To further verify the formation of the probe layer, the contact angle was determined by depositing approximately 3 μL droplets of deionized water onto the surface with a microliter syringe and allowing them to stabilize prior to measurement. To maintain measurement consistency, this process was conducted at least five times at various locations on the surface. Measurements were performed on both the surface coated solely with gold and the surface fully coated with the probe layer.

As previously noted, the PM3 system is employed to detect changes in the microcantilever's frequency. In this arrangement, a laser beam targets the backside of the microcantilever, is then reflected onto a four-quadrant photodiode, and the resulting output signal is utilized to record the variations in the microcantilever's frequency.

3. Results

The surface morphology of the microcantilever was analyzed using AFM before and after modification, illustrated in Fig. 2. Surface roughness values were calculated for the bare gold-coated microcantilever and for various modification layers. The surface modified with anti-PD-L1 exhibited higher roughness values compared to the bare gold-coated surface, suggesting the formation of a sensing layer on the microcantilever. The RMS roughness (σ_R) value for the bare gold surface

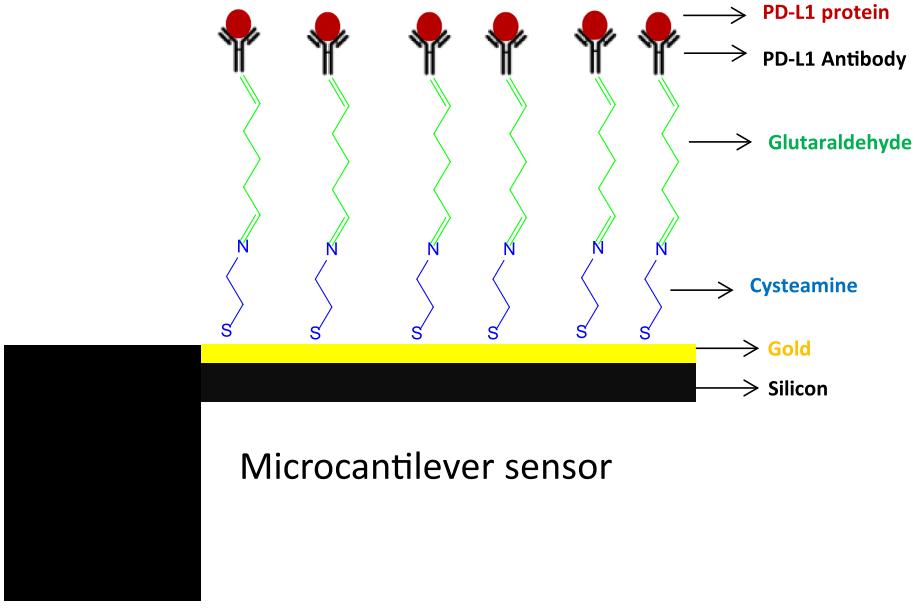

Fig. 1. Schematic representation of the microcantilever sensor modification process, detailing the steps involved in preparing and functionalizing the sensor for enhanced detection capabilities.

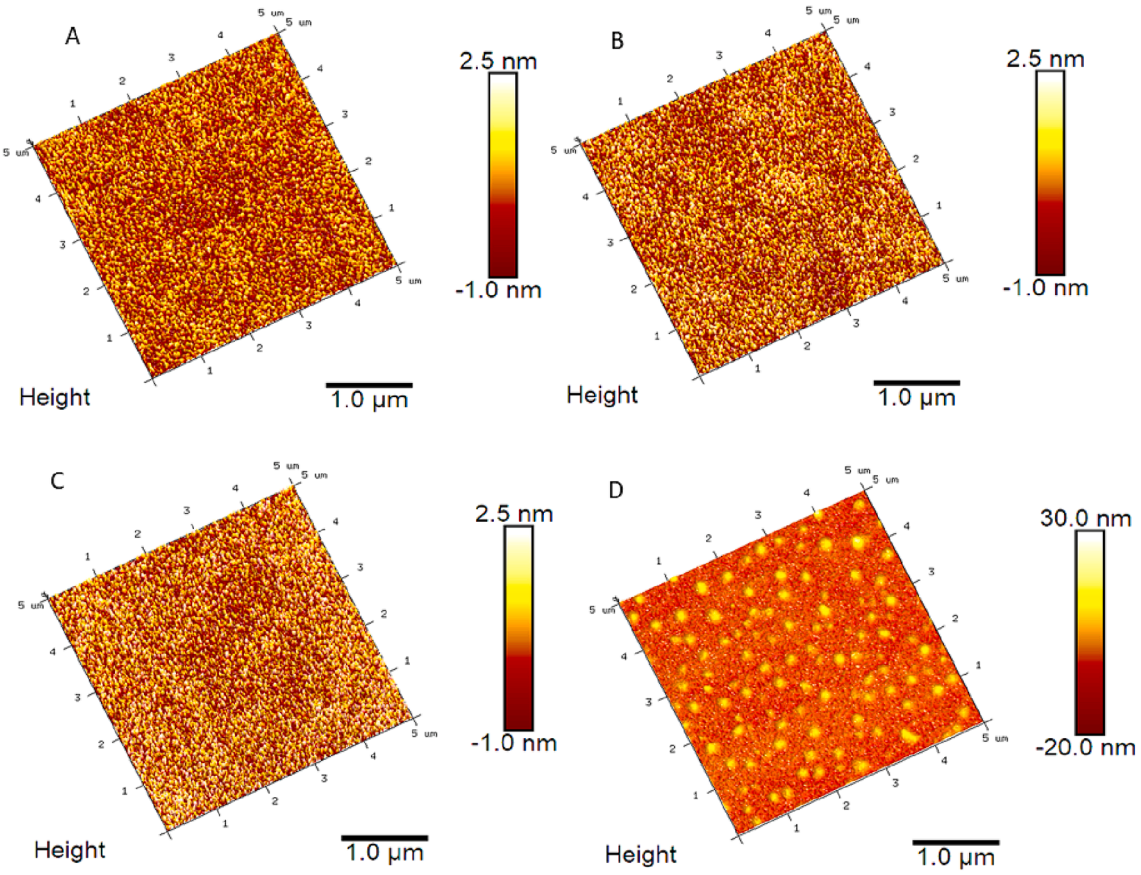

Fig. 2. 3D AFM images illustrating the sequential surface modification of a microcantilever sensor: (A) Bare-Au representing the unmodified state, (B) Au-Cysteamine showing the initial functionalization layer, (C) Au-Cysteamine-Glutaraldehyde indicating the addition of a crosslinker, and (D) Au-Cysteamine-Glutraldehyde-PD-L1 antibody depicting the final biofunctionalized surface ready for specific biomolecular interactions.

was calculated to be 0.78 nm ± 0.2 and 2.6 nm ± 0.3 for anti-PD-L1-functionalized surface. As shown in Fig. 2A–C, the Atomic Force Microscopy (AFM) images depict a two-step surface functionalization process. The first image shows a smooth, uniform layer of gold, which serves as the foundational interface for subsequent chemical modifications. Following this, the second image reveals the surface after functionalization with cysteamine, a crucial molecular linker. This stage is characterized by a noticeable change in surface texture, indicating the successful attachment of cysteamine to the gold layer. Cysteamine's role is pivotal, introducing functional groups that enable the binding of glutaraldehyde, which is intended for the subsequent attachment of antibodies. As can be observed in Fig. 2D, an increase in feature sizes is observed, indicating the attachment of anti-PD-L1 to the surface.

Fig. 3 shows the AFM images of the surfaces with PD-L1 attached to anti-PD-L1. The height of anti-PD-L1 /PD-L1 immobilized on the surface was slightly higher than that of only the antibody, confirming effective binding between the PD-L1 protein and anti-PD-L1.

The contact angle measurements, as depicted in Fig. 4, provide

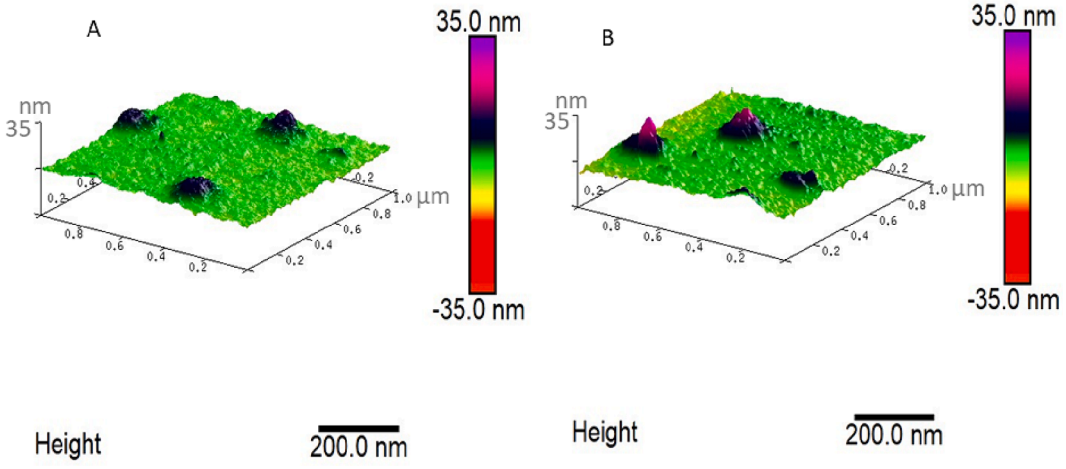

Fig. 3. AFM images of a gold surface functionalized by PD-L1 antibody probe layer: (A) before incubation in PD-L1 protein, showing the initial probe layer, and (B) after incubation in 50 ng/ml PD-L1 protein, illustrating changes in surface morphology due to specific protein binding.

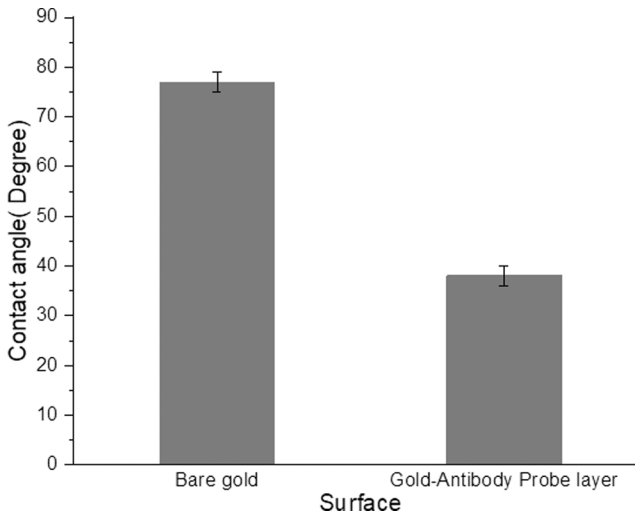

Fig. 4. Illustration of contact angle measurements depicting the hydrophilicity changes of a gold surface: before PD-L1 probe layer immobilization, showing the inherent contact angle of the bare surface, and after anti-PD-L1 probe layer immobilization, indicating the altered surface wetting properties due to the presence of the biomolecular layer. Error bars correspond to the relevant standard deviations.

additional evidence for the successful attachment of anti-PD-L1 to the surface. When modified with anti-PD-L1, the surface exhibited a contact angle decrease to approximately 38°, in contrast to approximately 76° for the bare gold-coated surface.

Fig. 5A illustrates the resonance frequency curves of a microcantilever when exposed to varying concentrations of PD-L1 proteins. The frequency shift was determined by subtracting the baseline resonance frequency (established before the binding of PD-L1 with anti-PD-L1) from the measured frequency after the binding occurred. Notably, there is a descending shift in resonance frequency corresponding to an increase in PD-L1 protein concentration. Fig. 5B further clarifies this relationship by showing the frequency shift relative to the PD-L1 protein concentration. The curve demonstrates a definitive trend where the frequency shift escalates with higher PD-L1 concentrations, confirming the cantilever's ability not just to detect these proteins but also to provide a quantitative assessment of their concentration. For example, at a concentration of 50 pg/ml, the frequency shift is around 5 Hz, and this shift escalates to approximately 35 Hz when the concentration increases to 500 ng/ml.

Fig. 6 shows the calibration curve for PD-L1 detection, depicting the correlation between the shift in resonance frequency and the logarithmically scaled PD-L1 concentration. This curve demonstrates that from 50 pg/ml to 500 ng/ml, a linear relationship exists between the resonance frequency shift and the logarithm of the PD-L1 concentration.

Fig. 7 illustrates the evaluation of the sensor's selectivity. Three distinct samples were tested: one containing only PBS (phosphate-buffered saline), a negative control solution, and a positive control solution. The negative control was a complex mixture consisting of fibrinogen, LDL (low-density lipoprotein) cholesterol, and cytomegalovirus antigens in PBS. In contrast, the positive control solution comprised the same components as the negative control but was additionally enriched with PD-L1. Fig. 7 demonstrates the sensor's response to different control samples. The negative control, which did not contain PD-L1, showed no significant shift in the sensor's resonance frequency compared to the samples treated with only PBS. Conversely, the

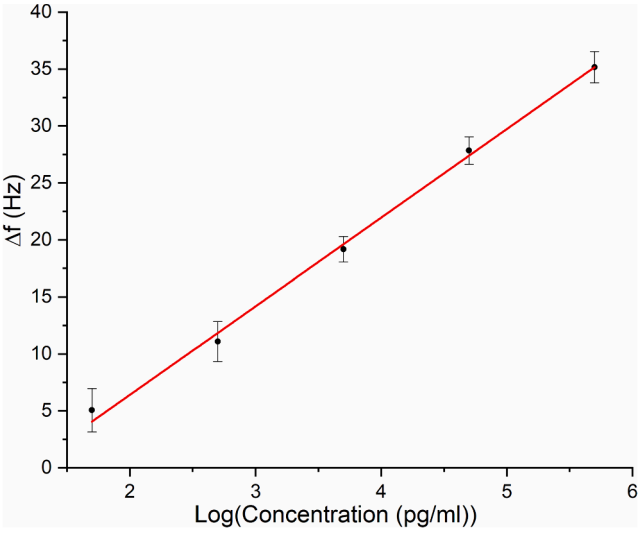

Fig. 6. Calibration curve depicting the resonance frequency shift against the logarithmic scale of PD-L1 concentration. The results demonstrate a linear relationship for PD-L1 detection within a specific concentration range, highlighting the sensor's sensitivity and dynamic range Error bars correspond to the relevant standard deviations.

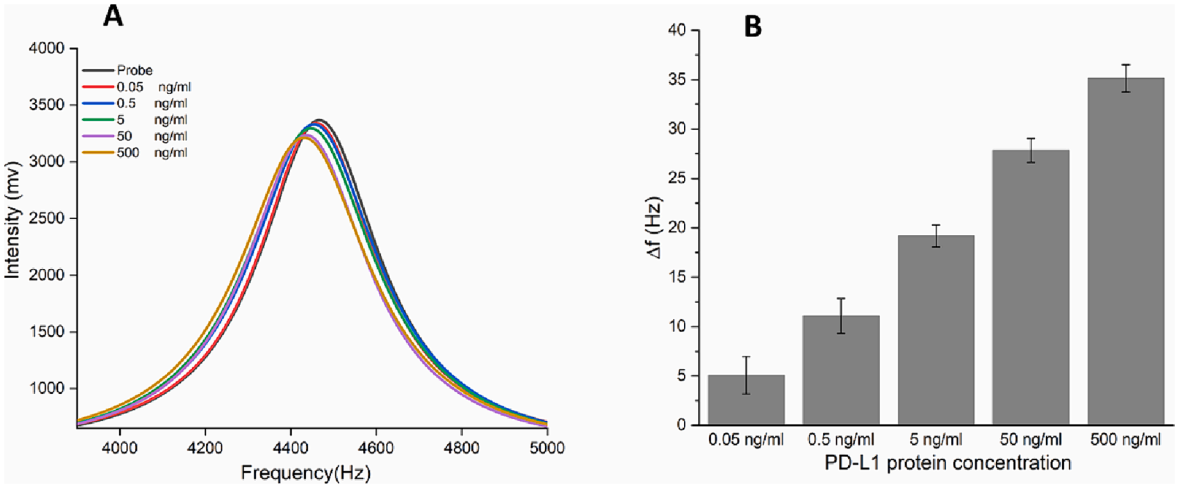

Fig. 5. (A) Resonance frequency curves for various PD-L1 concentrations, illustrating the sensor's response to incremental changes in PD-L1 presence. (B) Comparison of resonance frequency shift (Δf) of the sensor across various PD-L1 concentrations. The frequency shift is calculated as the average of eight replicates, and the error bars correspond to the standard deviation.

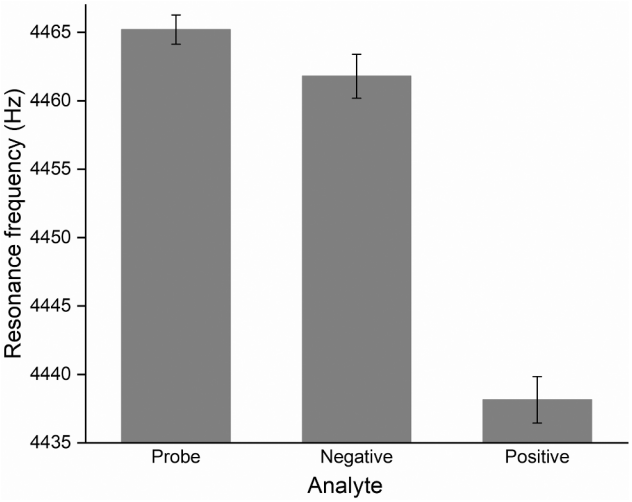

Fig. 7. Selectivity assessment of the sensor: The probe denotes the microcantilever modified with anti-PD-L1. The 'negative' represents the anti-PD-L1-modified microcantilever treated with a biomolecule mixture excluding PD-L1, whereas the 'positive' includes the same mixture with the addition of PD-L1. This comparison elucidates the sensor's specificity in distinguishing the presence of the target PD-L1 amidst a complex background. Error bars correspond to the respective standard deviations.

introduction of the positive control, which included PD-L1, resulted in a noticeable shift in the resonance frequency.

4. Discussion

The sensing layer is a critical element of biosensors, allowing for the specific detection of the target analyte. It is composed of biological recognition elements such as enzymes, antibodies, and DNA, which have the ability to selectively bind to the analyte of interest. When the analyte binds to the sensing layer, it induces a measurable change in physical properties such as mass, electrical conductivity, or optical characteristics. This change is then converted into a readable analytical signal by the biosensor's transducer component. To verify the formation of the sensing layer on the biosensor surface, two methods were utilized: contact angle measurements and AFM.

Contact angle measurements provided additional insights. If two surfaces exhibit different contact angle values for the same liquid, this indicates that the surfaces have different surface energies and interact differently with the liquid molecules. The contact angle is a measure of the wettability of a surface and depends on the relative intermolecular interactions between the liquid molecules (cohesive forces) and the interactions between the liquid and solid surface molecules (adhesive forces). The surface modified with anti-PD-L1 exhibits a lower contact angle compared to the non-modified surface. The difference in contact angles indicates the modified surface is more hydrophilic than the non-modified surface. The disparity could be attributed to variances in surface chemistry, roughness, contamination levels or heterogeneity between the two surfaces, indicating the establishment of a sensory layer on the microcantilever surface. This ties in well with observation about the roughness of the surface.

The AFM measured the surface roughness, and a significant difference in roughness values between the bare gold-coated microcantilever and the one modified with anti-PD-L1 suggests the successful formation of the sensing layer. The small features observed on the microcantilever surface after the attachment of anti-PD-L1 are further critical indicators, signifying the successful and correct attachment of the anti-PD-L1 molecules. This attachment is vital for the sensor's intended functionality, ensuring its accuracy and efficiency in target detection.

When PD-L1, the targeted analyte, comes into contact with the microcantilever's surface, it causes a measurable change in frequency. This change is largely attributed to the added mass effect. As the PD-L1 proteins bind to the probe layer on the microcantilever, they add extra mass, resulting in a reduced resonance frequency. This shift in frequency is a crucial measure of the microcantilever's sensitivity and its ability to analyze biomolecular interactions quantitatively. The sensor's detection limit was determined to be ~10 pg/ml. The efficacy of the PD-L1 sensor was assessed by testing solutions of PD-L1 at varying concentrations, all at room temperature. A strong linear relationship is observed between the frequency shift and the logarithm of the PD-L1 concentration. The sensor's detection limit was determined to be ~10 pg/ml. This outcome demonstrates that the sensor offers a straightforward and effective platform for detecting PD-L1. Although our sensor exhibits high sensitivity, other techniques like Surface-Enhanced Raman Spectroscopy (SERS) sensors demonstrate even greater sensitivity with a limit of detection limit at 100 fg/ml. Table 1. illustrates a list of different biosensing technologies used for the detection of PD-L1 and their corresponding limit of detection (LoD). The reported biosensor here is comparable to these technologies. However, the biosensor offers stability, portability and low-cost. In addition, the reported biosensor size is significantly smaller than the most reported biosensors in Table 1. Hence, the biosensor allows on-site detection of PD-L1 and other biomarkers.

Selectivity towards PD-L1 is a crucial characteristic of the sensor, significantly influenced by the specificity of the anti-PD-L1. In our study, we investigated the sensor's response to various potential interfering substances, encompassing proteins, antigens, and other biomolecules. The sensor shows a high affinity for PD-L1. This indicates a high level of specificity as the sensor did not falsely respond to other components in the mixture. This pronounced change confirms the sensor's capability to distinctly recognize and respond to PD-L1, even when it's amongst a variety of other biomolecules. The clear differential response between the negative and positive controls underscores the sensor's potential for precise and reliable detection in complex biological environments, making it a promising tool for diagnostic and research applications where specificity is paramount.

5. Conclusion

This study successfully demonstrated the potential of a microcantilever-based biosensor for the sensitive and specific detection of soluble Programmed Death Ligand 1 (sPD-L1), a biomarker crucial in cancer immunotherapy and prognosis. The biosensor, employing anti-PD-L1 as a sensing layer, capitalizes on the specific binding affinity between anti-PD-L1 and sPD-L1, translating the biomolecular interactions into a measurable shift in the microcantilever's resonance frequency. The surface modification was validated through AFM and contact angle measurements, confirming the successful establishment of the sensing layer. Results indicated a definitive, linear relationship between the frequency shift and the logarithm of PD-L1 concentration ranging from 50 pg/ml to 500 ng/ml, with a detection limit of

Table I
List of the reported PD-L1 detection techniques and their LoD.

Detection method	*LoD*	*Ref.*
Quartz Tuning Fork	8.26 pg/mL	(Algwati et al., 2023)
Fluorescent based aptasensor	9.40×10^4 particles/µl	(Feng et al., 2023)
Electrohydrodynamic biosensor	5 pg/mL	(Wuethrich et al., 2019)
Electrochemical aptasensor	36 particles/mL	(Chang et al., 2023)
Enzyme-linked immunosorbent assay (ELISA)	57 pg/ml	(Tiako Meyo et al., 2020)
Surface plasmon resonance-based biosensor	3.29 ng/ml	(Huang et al., 2021)
Cantilever-based biosensor	10.2 pg/mL	This work

approximately 10 pg/ml. This sensitivity, coupled with the biosensor's ability to discriminate between complex biological mixtures, underscores its potential for early cancer diagnosis and monitoring immunotherapy efficacy. The distinct response between the negative and positive controls further confirms the high selectivity and reliability of this biosensing approach. The biosensor presents a promising, economical, and user-friendly tool for early cancer diagnosis and evaluation of immunotherapy. Its high sensitivity, specificity, and capability to operate in complex biological environments pave the way for personalized and effective cancer treatments.

The microcantilever-based biosensor demonstrated promising sensitivity and specificity for the detection of PD-L1. Despite these encouraging results, the transition from laboratory settings to actual clinical application warrants further investigation. The biosensor's performance with real patient samples presents a complex challenge, influenced by the inherent variability in biological samples due to factors such as dietary habits, medication intake, and the underlying disease state. Additionally, the integration of this novel technology into existing clinical workflows remains a crucial step towards its widespread adoption. To overcome these obstacles, our future research endeavors will concentrate on extensive clinical validation across a diverse array of patient samples to ascertain the biosensor's diagnostic precision and reliability. Furthermore, efforts will be directed towards refining the biosensor's design to enhance its portability, user-friendliness, and overall robustness, ensuring its suitability for routine clinical use. A significant focus will be placed on the integration of microfluidic technology with the microcantilever sensor, which is anticipated to streamline sample handling.

Declaration of Competing Interest

The authors declare that they have no known competing financial interests or personal relationships that could have appeared to influence the work reported in this paper.

Acknowledgement

Funding is provided by the Deputyship for Research & Innovation, Ministry of Education in Saudi Arabia through the project no. (IFKSUDR_H184).

References

Algwati, M., Q. T. Ain, K. Alzahrani, A. Assaifan, T. Neairat, N. Alarifi, A. Alarifi, A. Alshamsan, A. Alodhayb and H. Albrithen (2023). "Label Free Detection of Programmed Death Ligand 1 Protein Biomarker by Quartz Tuning Fork-Based Biosensor." Journal of The Electrochemical Society.

Alzahrani, K.E., Alodhayb, A., Algwati, M., Alanazi, A.F., Ain, Q.T., Assaifan, A.K., Manoharadas, S., Alshammari, A., Alswieleh, A., Albrithen, H., 2021. Nanomechanical detection of bacteria–bacteriophage interactions using microchannel microcantilevers. J. Electrochem. Soc. 168 (8), 087509.

Alzahrani, K.E., Al-Gawati, M., Assaifan, A.K., Alodhayb, A., Alotaibi, K., Alswieleh, A., Albrithen, H., Alanazi, A.F., 2023a. Label free detection of vitamin D by microcantilever-based aptasensor. J. King Saud Univ.-Sci. 35 (10), 102951.

Alzahrani, K.E., Assaifan, A.K., Al-Gawati, M., Alswieleh, A.M., Albrithen, H., Alodhayb, A., 2023b. Microelectromechanical system-based biosensor for label-free detection of human cytomegalovirus. IET Nanobiotechnol. 17 (1), 32–39.

Bray, F., Ferlay, J., Soerjomataram, I., Siegel, R.L., Torre, L.A., Jemal, A., 2018. Global cancer statistics 2018: GLOBOCAN estimates of incidence and mortality worldwide for 36 cancers in 185 countries. CA Cancer J. Clin. 68 (6), 394–424.

Chang, B., Huang, T., Wei, H., Shen, L., Zhu, D., He, W., Chen, Q., Zhang, H., Li, Y., Huang, R., 2019. The correlation and prognostic value of serum levels of soluble programmed death protein 1 (sPD-1) and soluble programmed death-ligand 1 (sPD-L1) in patients with hepatocellular carcinoma. Cancer Immunol. Immunother. 68, 353–363.

Chang, L., Wu, H., Chen, R., Sun, X., Yang, Y., Huang, C., Ding, S., Liu, C., Cheng, W., 2023. Microporous PdCuB nanotag-based electrochemical aptasensor with au@CuCl2 nanowires interface for ultrasensitive detection of PD-L1-positive exosomes in the serum of lung cancer patients. J. Nanobiotechnol. 21 (1), 86.

Chen, Y., Wang, Q., Shi, B., Xu, P., Hu, Z., Bai, L., Zhang, X., 2011. Development of a sandwich ELISA for evaluating soluble PD-L1 (CD274) in human sera of different ages as well as supernatants of PD-L1+ cell lines. Cytokine 56 (2), 231–238.

Ding, Y., Sun, C., Li, J., Hu, L., Li, M., Liu, J., Pu, L., Xiong, S., 2017. The prognostic significance of soluble programmed death ligand 1 expression in cancers: a systematic review and meta-analysis. Scand. J. Immunol. 86 (5), 361–367.

Etayash, H., Jiang, K., Azmi, S., Thundat, T., Kaur, K., 2015. Real-time detection of breast cancer cells using peptide-functionalized microcantilever arrays. Sci. Rep. 5 (1), 13967.

Feng, J., Jia, L., Pan, W., Fan, Y., Guo, J., Luo, T., Liu, C., Wang, W., Zheng, L., Li, B., 2023. Rapid and efficient fluorescent aptasensor for PD-L1 positive extracellular vesicles isolation and analysis: EV-ANCHOR. Chem. Eng. J. 465, 142811.

Feng, M., Xiong, G., Cao, Z., Yang, G., Zheng, S., Song, X., You, L., Zheng, L., Zhang, T., Zhao, Y., 2017. PD-1/PD-L1 and immunotherapy for pancreatic cancer. Cancer Lett. 407, 57–65.

Ferlay, J., Colombet, M., Soerjomataram, I., Parkin, D.M., Piñeros, M., Znaor, A., Bray, F., 2021. Cancer statistics for the year 2020: an overview. Int. J. Cancer 149 (4), 778–789.

Festino, L., Botti, G., Lorigan, P., Masucci, G.V., Hipp, J.D., Horak, C.E., Melero, I., Ascierto, P.A., 2016. Cancer treatment with anti-PD-1/PD-L1 agents: is PD-L1 expression a biomarker for patient selection? Drugs 76, 925–945.

Frigola, X., Inman, B.A., Lohse, C.M., Krco, C.J., Cheville, J.C., Thompson, R.H., Leibovich, B., Blute, M.L., Dong, H., Kwon, E.D., 2011. Identification of a soluble form of B7–H1 that retains immunosuppressive activity and is associated with aggressive renal cell carcinoma. Clin. Cancer Res. 17 (7), 1915–1923.

Gopinath, P., Anitha, V., Mastani, S.A., 2015. Microcantilever based biosensor for disease detection applications. J. Med. Bioeng. 4 (4), 34.

Hu, J., Zhang, Z.-H., Zhu, Z., Chen, J., Hu, X., Chen, H., 2021. Specific intracellular binding peptide as sPD-L1 antibody mimic: robust binding capacity and intracellular region specific modulation upon applied to sensing research. Biosens. Bioelectron. 185, 113269.

Huang, X., Zhang, Z.-H., Chen, J., Mao, Z., Zhu, H., Liu, Y., Zhu, Z., Chen, H., 2021. One dimensional magneto-optical nanocomplex from silver nanoclusters and magnetite nanorods containing ordered mesocages for sensitive detection of PD-L1. Biosens. Bioelectron. 189, 113385.

Jiang, Y., Chen, M., Nie, H., Yuan, Y., 2019. PD-1 and PD-L1 in cancer immunotherapy: clinical implications and future considerations. Hum. Vaccin. Immunother. 15 (5), 1111–1122.

Kim, H.H., Jeon, H.J., Cho, H.K., Cheong, J.H., Moon, H.S., Go, J.S., 2015. Highly sensitive microcantilever biosensors with enhanced sensitivity for detection of human papilloma virus infection. Sens. Actuators B 221, 1372–1383.

Kruger, S., Legenstein, M.-L., Rösgen, V., Haas, M., Modest, D.P., Westphalen, C.B., Ormanns, S., Kirchner, T., Heinemann, V., Holdenrieder, S., 2017. Serum levels of soluble programmed death protein 1 (sPD-1) and soluble programmed death ligand 1 (sPD-L1) in advanced pancreatic cancer. Oncoimmunology 6 (5), e1310358.

Longo, G., Alonso-Sarduy, L., Rio, L.M., Bizzini, A., Trampuz, A., Notz, J., Dietler, G., Kasas, S., 2013. Rapid detection of bacterial resistance to antibiotics using AFM cantilevers as nanomechanical sensors. Nat. Nanotechnol. 8 (7), 522–526.

Mahoney, K.M., Freeman, G.J., McDermott, D.F., 2015. The next immune-checkpoint inhibitors: PD-1/PD-L1 blockade in melanoma. Clin. Ther. 37 (4), 764–782.

Mansouri, V., Beheshtizadeh, N., Gharibshahian, M., Sabouri, L., Varzandeh, M., Rezaei, N., 2021. Recent advances in regenerative medicine strategies for cancer treatment. Biomed. Pharmacother. 141, 111875.

Patel, S.P., Kurzrock, R., 2015. PD-L1 expression as a predictive biomarker in cancer immunotherapy. Mol. Cancer Ther. 14 (4), 847–856.

RáGonšales, V., JustináGooding, J., 2021. Ultrasensitive detection of programmed death-ligand 1 (PD-L1) in whole blood using dispersible electrodes. Chem. Commun. 57 (20), 2559–2562.

Reinemann, C., Stoltenburg, R., Strehlitz, B., 2009. Investigations on the specificity of DNA aptamers binding to ethanolamine. Anal. Chem. 81 (10), 3973–3978.

Reza, K.K., Sina, A.A.I., Wuethrich, A., Grewal, Y.S., Howard, C.B., Korbie, D., Trau, M., 2019. A SERS microfluidic platform for targeting multiple soluble immune checkpoints. Biosens. Bioelectron. 126, 178–186.

Ricciardi, C., Fiorilli, S., Bianco, S., Canavese, G., Castagna, R., Ferrante, I., Digregorio, G., Marasso, S.L., Napione, L., Bussolino, F., 2010. Development of microcantilever-based biosensor array to detect Angiopoietin-1, a marker of tumor angiogenesis. Biosens. Bioelectron. 25 (5), 1193–1198.

Tiako Meyo, M., Jouinot, A., Giroux-Leprieur, E., Fabre, E., Wislez, M., Alifano, M., Leroy, K., Boudou-Rouquette, P., Tlemsani, C., Khoudour, N., 2020. Predictive value of soluble PD-1, PD-L1, VEGFA, CD40 ligand and CD44 for nivolumab therapy in advanced non-small cell lung cancer: a case-control study. Cancers 12 (2), 473.

Wang, S., Wang, J., Zhu, Y., Yang, J., Yang, F., 2015. A new device for liver cancer biomarker detection with high accuracy. Sens. Bio-Sens. Res. 4, 40–45.

Wuethrich, A., Rajkumar, A.R., Shanmugasundaram, K.B., Reza, K.K., Dey, S., Howard, C.B., Sina, A.A.I., Trau, M., 2019. Single droplet detection of immune checkpoints on a multiplexed electrohydrodynamic biosensor. Analyst 144 (23), 6914–6921.

Xing, Y., Liu, J., Sun, S., Ming, T., Wang, Y., Luo, J., Xiao, G., Li, X., Xie, J., Cai, X., 2021. New electrochemical method for programmed death-ligand 1 detection based on a paper-based microfluidic aptasensor. Bioelectrochemistry 140, 107789.

Xing, Y., Liu, J., Luo, J., Ming, T., Yang, G., Sun, S., Xu, S., Li, X., He, E., Kong, F., 2022. A dual-channel intelligent point-of-care testing system for soluble programmed death-1 and programmed death-ligand 1 detection based on folding paper-based immunosensors. ACS Sensors 7 (2), 584–592.

Yang, F., Wang, J.F., Wang, Y., Liu, B., Molina, J.R., 2021. Comparative analysis of predictive biomarkers for PD-1/PD-L1 inhibitors in cancers: developments and challenges. Cancers 14 (1), 109.